

OPEN

A next generation setup for pre-fractionation of non-denatured proteins reveals diverse albumin proteoforms each carrying several post-translational modifications

Heidrun Rhode¹, Petra Muckova¹, Rita Büchler^{1,6}, Sindy Wendler^{1,7}, Bärbel Tautkus¹, Michaela Vogel¹, Thomas Moore², Julian Grosskreutz³, Andree Klemm⁴ & Mary Nability⁵

Proteomic biomarker search requires the greatest analytical reproducibility and detailed information on altered proteoforms. Our protein pre-fractionation applies orthogonal native chromatography and conserves important features of protein variants such as native molecular weight, charge and major glycans. Moreover, we maximized reproducibility of sample pre-fractionation and preparation before mass spectrometry by parallelization and automation. In blood plasma and cerebrospinal fluid (CSF), most proteins, including candidate biomarkers, distribute into a multitude of chromatographic clusters. Plasma albumin, for example, divides into 15-17 clusters. As an example of our technique, we analyzed these albumin clusters from healthy volunteers and from dogs and identified cluster-typical modification patterns. Renal disease further modifies these patterns. In human CSF, we found only a subset of proteoforms with fewer modifications than in plasma. We infer from this example that our method can be used to identify and characterize distinct proteoforms and, optionally, enrich them, thereby yielding the characteristics of proteoform-selective biomarkers.

A major challenge in the search for proteomic biomarkers is the low reproducibility among studies. There are several likely reasons for this low reproducibility most of which originate from experimental design or methodology^{1,2} such as insufficient proteome coverage and low workflow precision^{3,4}. It is also difficult to obtain longitudinal samples and perform multidisciplinary studies¹. However, another significant cause is the biological variability of protein expression and modification⁵⁻⁸. Protein modifications are variable among healthy individuals and diseases further alter the diversity of multiple proteoforms⁸ producing dysfunctional or even toxic entities^{9,10}. Therefore, it is illogical to expect that it is possible to produce a reliably usable biomarker from an entire protein family deduced from a few tryptic peptides^{11,12}. This role is more reasonably fulfilled by one or multiple distinct proteoforms.

To identify and quantify specific proteoform biomarkers among the many and varied modifications possible, new experimental ideas and settings are required because the common shotgun and bottom-up approaches are insufficient for this purpose¹³. More suitable for identifying disease specific modifications are comprehensive, unbiased, and precise sample pre-fractionation methods on the protein level^{7,8,12}, combined with sophisticated data analyses.

¹Institute of Biochemistry I, Nonnenplan 2-4, University Hospital Jena, 07740, Jena, Germany. ²Analytik Jena, Konrad-Zuse-Str.1, 07745, Jena, Germany. ³Department of Neurology, Am Klinikum 1, University Hospital Jena, 07747, Jena, Germany. ⁴KfH Kuratorium für Dialyse und Nierentransplantation e.V., Ernst-Ruska-Ring 19, 07745, Jena, Germany. ⁵Department of Veterinary Pathobiology, College of Veterinary Medicine, 4467 TAMU, Texas A&M University, College Station, TX, 77843-4467, Texas, USA. ⁶Present address: Pharmachem Straße 1, Pharmachem Pößneck GmbH & Co. KG, 07381, Pößneck, Germany. ⁷Present address: Institute of Microbiology, Am Klinikum 1, University Hospital Jena, 07747, Jena, Germany. Correspondence and requests for materials should be addressed to H.R. (email: Heidrun.Rhode@med.uni-jena.de)

Received: 25 January 2019

Accepted: 29 July 2019

Published online: 13 August 2019

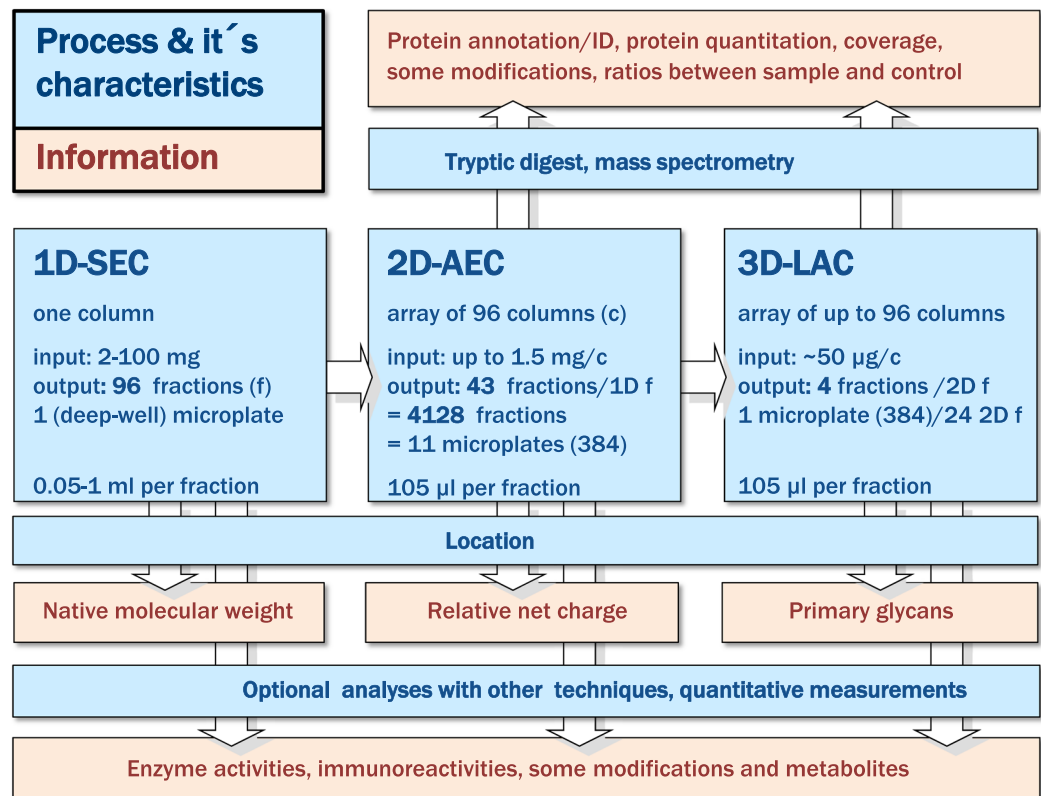


Figure 1. Scheme of the workflow. Blue: methods, processes and some characteristics; orange: potential information derived from the location of identified constituents and from additional analyses of sub-fractions.

We therefore developed an unbiased protein pre-fractionation workflow using non-denaturing multidimensional chromatography. We adapted the workflow for the proteomic analysis of body fluids without any depletion. This workflow therefore allows the characterization of the entire proteome. The combination of parallel liquid handling, microplate format, and automation ensures maximum velocity, precision and reproducibility¹⁴. Moreover, the workflow inherently produces highly characteristic sub-fractions. This thereby preserves information on the native molecular weight (Mw, indicating complex formation, large posttranslational modifications (PTM), and fragmentation), charge (- PTM and conformation), and lectin affinity (- major types of glycans). The immune reactivity and biological activities of the proteoforms can also be analyzed in our native sub-fractions when required¹⁵. Such information is beneficial for identifying specific proteoform biomarkers as well as for their validation.

As expected, we showed that the majority of plasma proteins appear in multiple chromatographic clusters^{7,16,17}. It is necessary to determine the probable reasons for this heterogeneity in order to identify biomarkers that are highly specific for particular diseases. A principal reason is that different proteoforms are characterized by different splice variants and PTM. In addition, however, it is necessary to consider the role of fragmentation and of complex formation with proteins and metabolites. Since albumin is the dominant plasma protein and is not known to be glycosylated or otherwise functionally modified but might be altered in the body by various processes¹⁸, we used it as an example for characterizing the capabilities of our workflow. To provide proof of principle, we searched albumin heterogeneity for various PTM.

Results

Characteristics of the separation procedure. Our method orthogonally combined size exclusion chromatography (SEC, first dimension, 1D), followed by anion exchange (AEC, 2D) and, optionally, lectin affinity (LAC, 3D) chromatography (Fig. 1). After serial 1D-fractionation, all further procedures were performed in microplate format. Beginning with 2D-fractionation, parallelization and automation was achieved for separation, preparation and analyses. Our automated workstation (Fig. 2a) enabled automated multichannel pipetting and robotic handling of microplates, reservoirs, and micro-column arrays, previously visualized by video¹⁶. For all fractionation processes, hit picking and analytics were controlled by adapted software packages. We developed several tools to maximize compatibility, throughput, recovery and precision of the preparation steps. We based protein recoveries from the corresponding load into liquid sub-fractions on UV measurements.

Native size exclusion chromatography enabled high protein input. Our first step, 1D-SEC, was characterized by the greatest reproducibility for reference peaks of UV-absorbing material (Supplementary Fig. 1, Table 1) regarding height and retention (elution volume). This initial step determined the scale of protein input

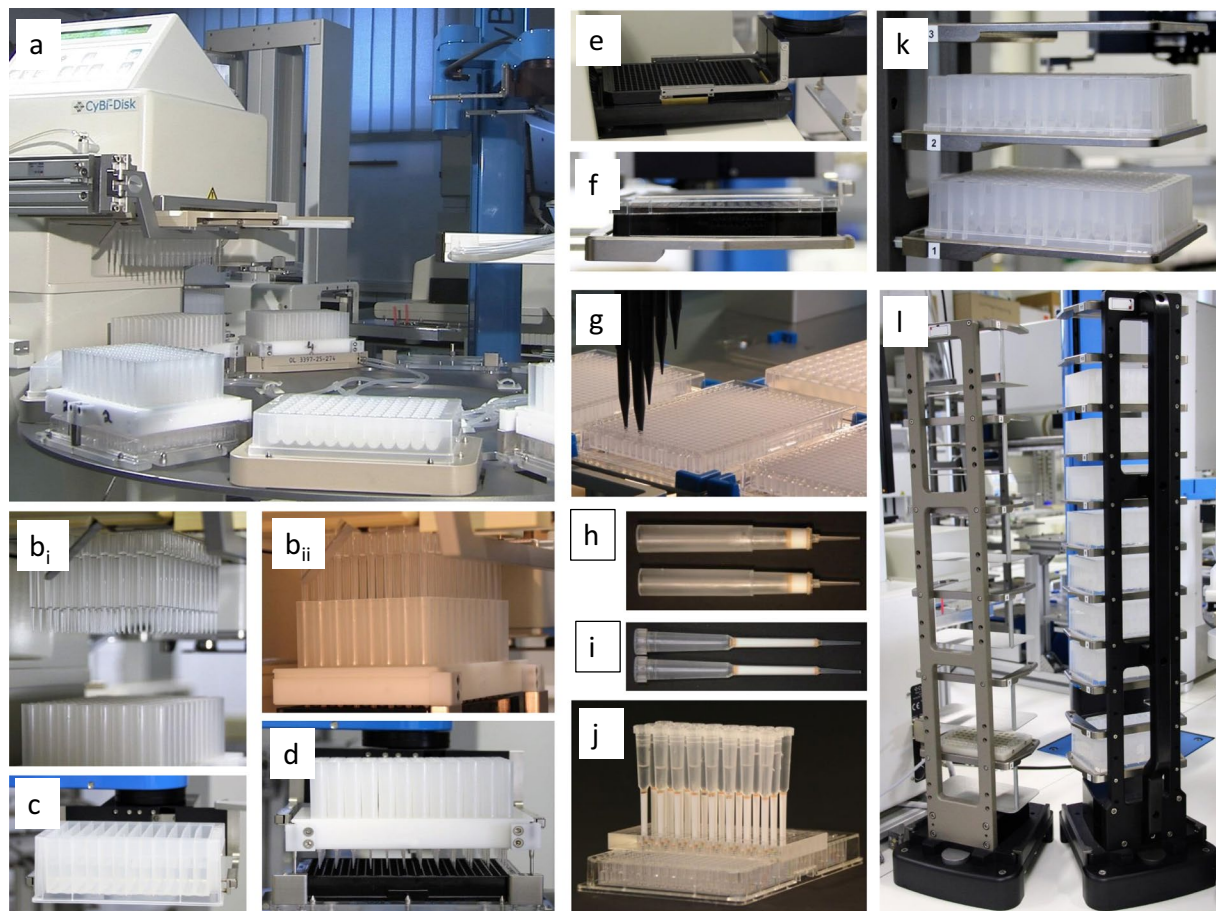


Figure 2. Devices and tools for automated and parallelized 2D-AEC and 3D-LAC. **(a)** Overview of our platform with the first liquid handler (used for the application of samples and elution solvents), the disc (carrying four 2D-column arrays and microplates containing 1D-fractions), and the robot for the automated handling of microplates, column arrays, tip racks, elution solvents, and microplate lids. **(b–l)** some details of chromatographic processing. **(b)** First liquid handler; 96 1D-fractions are pipetted onto the 2D (AEC)-column array (**b_i**: tips above columns, **b_{ii}**: tip position for discharging). **(c)** A reservoir containing one elution solvent is transported to the disc. **(d)** The column array is adjusted to the microplate. **(e)** Automatic readout of one 384-well microplate containing four 2D-fractions from each of the 96 1D-fractions; **(f)** Automatic sealing before moving into a refrigerator; **(g)** Second liquid handler; hit picking and reformatting of fractions; **(h)** Micro columns for 2D-AEC; **(i)** Micro columns for 3D-LAC; **(j)** Parallel 3D (LAC)-chromatography on 24 micro columns; **(k)** Stacker with two sample plates (96 1D-fractions of two samples); **(l)** Stacker for tip racks (left) and reservoirs of elution solvents (right).

(from 2 to more than 100 mg) and the expected range of molecular weight (from 2 to 1000 kDa). As expected, the recovery of UV-absorbing material was ~100%. Thus, the entire protein content (>30 kDa) of blood plasma (mean 93.7, SD 2.7% of the UV-absorbing material, cf. Supplementary Fig. 1) was completely separated from the intrinsic low molecular weight peptidome (<6 kDa).

Micro-column arrays provided truly parallel, automated and precise fractionation. No commercially available micro-columns for parallelized chromatography met all the requirements for volumes of 1D- and 2D-fractions, binding capacity, compatibility to 384-well microplates, free-flow elution of tunable elution rate, and precision. Therefore, we had to develop and optimize these tools ourselves. We made our own single columns and column arrays (Fig. 2d,j). We used empty SPE cartridges for AEC (Fig. 2h) and modified pipette tips for LAC (Fig. 2i). AEC runs over 100 μ L Toyopearl DEAE-650M (Tosoh Bioscience GmbH, Stuttgart, Germany) and LAC over 70 μ L Toyopearl AF-Tresyl 650 M (Tosoh Bioscience GmbH) modified with Concanavalin A (ConA, Sigma-Aldrich, C7275) and wheat germ agglutinin (WGA, Sigma-Aldrich, L9640)¹⁴. UV-absorbing material was recovered at mean 97.1, SD 11.2% with 3.8% CV after 2D fractionation and mean 88.8, SD 3.6% and 5.1% CV after 3D-fractionation¹⁴.

Parallel medium exchange by dialysis reliably produced compatibility with subsequent steps. Dialysis ensured compatibility of 1D-sub-fractions with 2D-AEC. It also removed sugars from 3D-sub-fractions and superfluous reagents from all sub-fractions after denaturation and modification prior to tryptic digest and mass spectrometry (MS). To perform medium exchange, we selected parallelized microdialysis

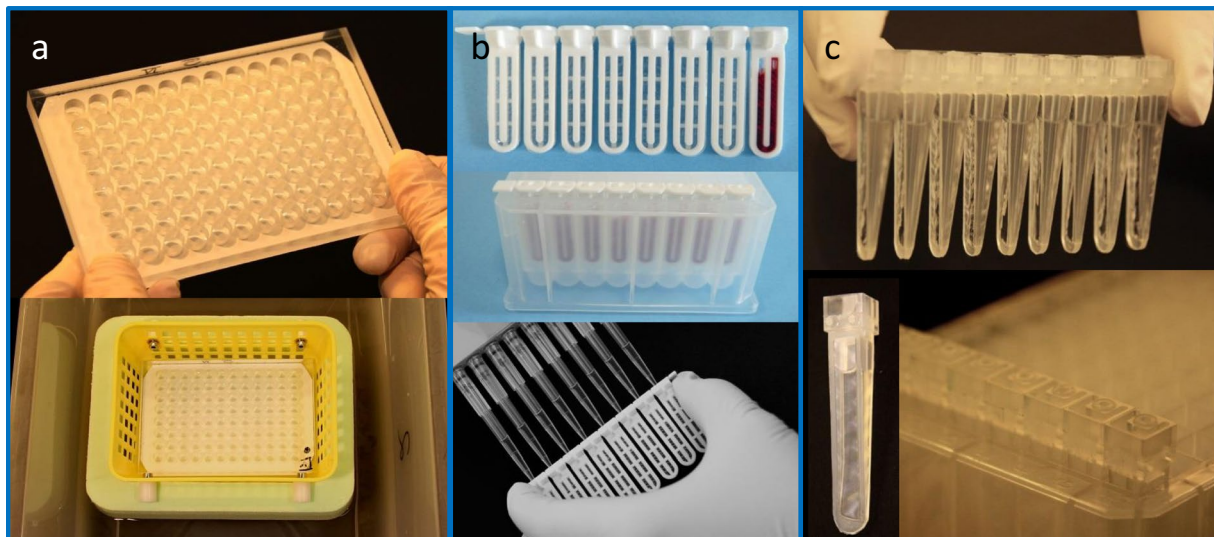


Figure 3. Parallel medium exchange applying three variants of suitable microdialysis tools. (a) Plate made in-house with 96 holes (250 μ L) equipped with a semipermeable membrane (Merck Millipore, VCWP14250), applied for lowering the ionic strength of 1D-fractions before 2D-AEC; (b) Xpress Micro Dialyzer MD100 (Fa. Scienova Inc.^{20,21}), ~30–100 μ L, applied for the removal of reagents and medium exchange before tryptic digest and MS; (c) Microdialyzer (still prototypic¹⁹), ~10–550 μ L, highest versatility, recovery and precision, applicable to all medium exchange steps of the entire workflow.

and developed various tools (Fig. 3)^{19,20,14,21} suitable for ensuring comprehensiveness and non-selectivity (see also <https://www.scienova.com>). For this method, only liquid handling was required, so guaranteeing high through-put, automation, and high precision. With the tool in Fig. 3a we routinely prepared 1D-sub-fractions for 2D-AEC. All tools achieved high protein recovery determined applying model proteins (bovine serum albumin (BSA), hemoglobin) and sample volumes of 100 μ L recoveries (e.g. mean 93.1, SD 1.3%²¹ (tool in Fig. 3b); mean 100.8, SD 0.01%¹⁹ (tool in Fig. 3c)). Moreover, the tool in Fig. 3c was applicable to a wide range of sample volumes (from 10 to nearly 600 μ L) with similar quality characteristics and it can be processed with various multichannel pipettes, including robots.

Our automated platform executed laborious repeated cycles of parallel chromatography. We iteratively developed our automated platform^{14,22}. With its current design (Fig. 2a) and its constituent tools (Figs 2 and 3), we were able to parallel process four samples through 2D-fractionation within three days (successive 1D SEC: two days including column calibration; parallel 2D AEC: one day including the medium exchange needed before AEC). Additional time was required for 3D-separation, tryptic digest, and MS. Our fractionation applied repeated process cycles with the selection of the target microplate, precise pipetting of fractions and of elution solvents on micro-columns, followed by complete flow-through and read out. 1D-sub-fractions were retrieved by the first liquid handler (Fig. 2a). The column arrays were adjusted to one partition of a microplate (Fig. 2d). The flow-through followed gravity without any support after a short initial pneumatic push (video in¹⁶). Elution solvents produced a stepwise gradient with increasing ionic strength¹⁴ (cf. Fig. 4c). From each 1D-fraction, four 2D-fractions were collected within one microplate. All successively filled microplates were instantly and automatically read (Fig. 2e), sealed, and transferred to the refrigerator (Fig. 2f). The platform can also, in principle, perform LAC. Picking and reformatting of fractions for subsequent preparation or MS was performed by the second liquid handler with 8 independent channels (Fig. 2g).

Examples of verified biomarkers. Applications of our methods showed versatility and high protein yield of plasma proteins from humans, cattle, goats, dogs and mice, and from human CSF (cf. Supplementary Tab. 1). The number of proteins identified in human samples is similar to that of current studies applying various proteomic approaches (e.g.^{23–25}). For example, from pooled human CSF, we were able to identify 5185 non-redundant proteins supported by ≥ 1 peptides and 1691 by ≥ 2 peptides. We also applied our method to the search for biomarkers of severe inflammation or sepsis, renal failure, Alport syndrome^{17,26–28}, and psoriasis¹⁶. In these searches, we obtained several candidate markers with significantly altered protein concentrations inferred from MS data. We validated several of these using immunoassays.

It must be noted that we consistently identified not only one but several chromatographic clusters for the majority of altered proteins, some of which demonstrated opposite directions of alteration. Sometimes we were unable to verify the main alteration of such biomarker candidates by commercial ELISA^{6,7} rather than one out of a minor cluster¹⁶. We are currently searching for the probable reasons for this heterogeneity of our biomarkers. We were able, using the facilities of the Proteome Discoverer[®] (see Online Methods), to uncover several interesting PTM for a variety of clusters of plasma proteins (patent sensitive data not shown). Below, we discuss our results for albumin, using it as an example of a typical eukaryotic protein.

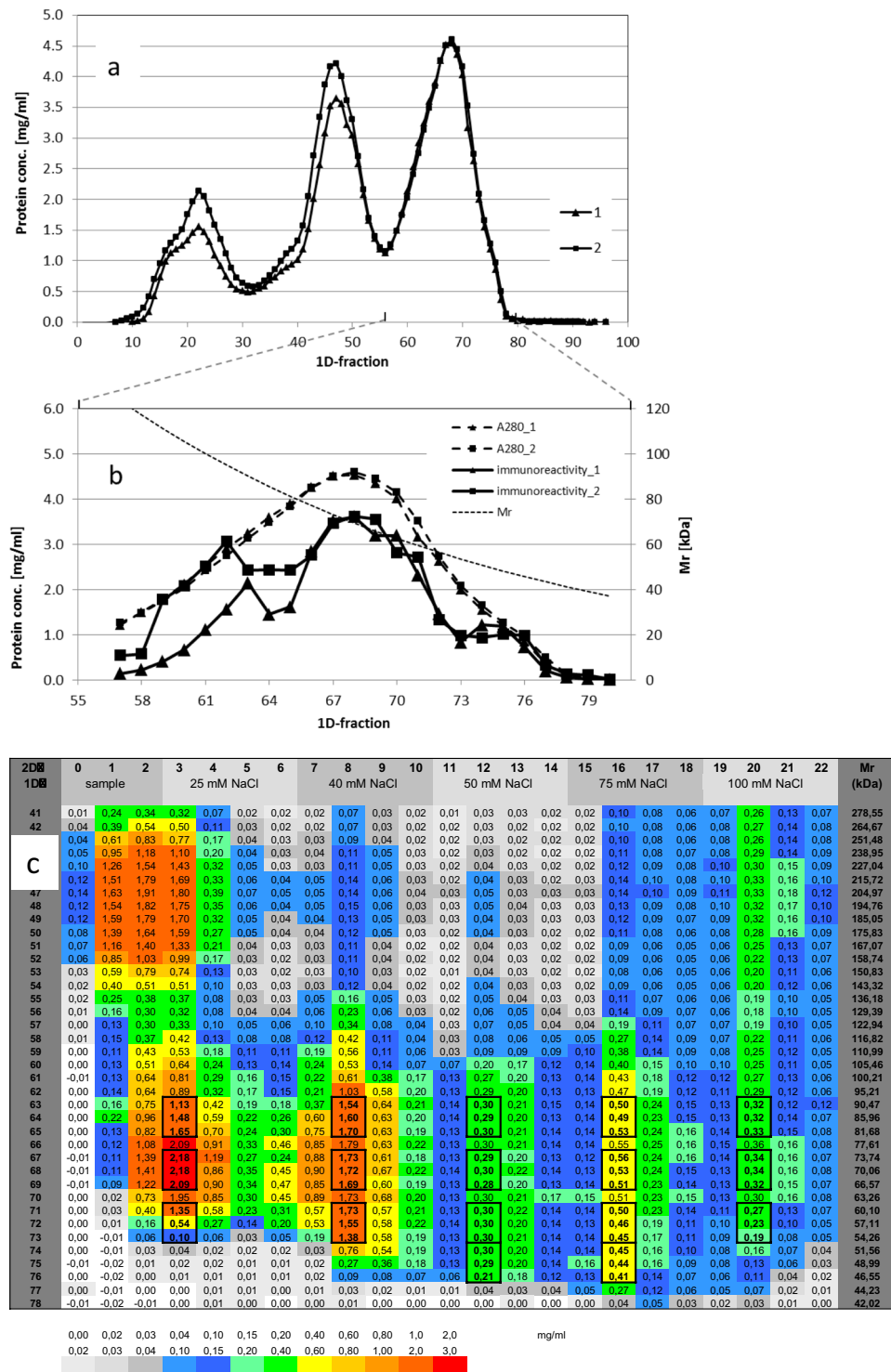


Figure 4. Protein separation after 1D-SEC and 2D-AEC. **(a)** Protein distribution after 1D-SEC of two samples from healthy male volunteers; section of all proteins above 30 kDa (A₂₈₀; cf. Supplementary Fig. 1). One mL of EDTA plasma was injected and separated on a HiLoad Superdex™ 200 column (16/60, GE Healthcare) in 10 mM Tris-HCl containing 150 mM NaCl (pH 7.4) and 1 mM EDTA at 17 °C. After the void volume 96 fractions of 1 mL were collected using a flow rate of 1 mL/min. Column calibration was performed as previously described¹⁴. **(b)** Albumin concentrations after 1D-SEC determined by ELISA^{15,26}; Section of 1D sub-fractions. **(c)** Section of 2D-sub-fractions containing serum albumin from sample 1 (see a). The entire protein distribution is reported elsewhere¹⁴. First column: number of 1D-fraction; last column: molecular weight according column calibration; first line: number of 2D-sub-fraction; second line: designation of sample and concentration of NaCl in the elution solvent 10 mM Tris-HCl, pH 7.4¹⁴. Frames indicate pooling from these fractions for PTM analysis. Total fractional concentrations of proteins were calculated from A₂₈₀ using BSA as standard and are given by values (mg/mL) and color code.

Albumin is a pure protein and not enzymatically modified but showing at least 17 proteoforms in blood plasma from human volunteers. We found albumin consistently highly heterogeneous in all of our blood samples from both patients and healthy control individuals^{16,17,26,27}, just as many other plasma proteins are. After 1D-SEC, immune reactive albumin reproducibly separated into three distinct peaks with apparent molecular weights of ~90–95 kDa, ~69–73 kDa, and ~50 kDa (Fig. 4a,b). Moreover, the low Mw form showed the strongest decline in patients suffering from sepsis²⁶. As many as 17 chromatographic clusters of this protein were produced after 2D-AEC (Fig. 4c). We analysed pools of 2D-sub-fractions of each cluster using the Proteome Discoverer[®], as indicated by boxes (Fig. 4c) (cf. Methods).

Each proteoform of serum albumin showed its own individual number and pattern of modifications. We were, in fact, able to identify several modifications, such as deamidation (R, N, Q), N-glycation (the majority on K, a few also predicted on R and Q), palmitoylation (S, K, T) and palmitoleylation (S, K), myristoylation (K), octanoylation (S, T), decanoylation (S, T), ethylation (E, K), acetylation (H, K, S, T, Y), methylation (D, E, H, I, K, L, N), dimethylation (K, N, R), propionylation (S, K), succinylations (K), carboxylation (K, E, D), carbamoylation (K), carboxymethylation (K), carboxyethylation (K), and phosphorylations (T, S, Y) and guanidylations (K).

To compare the results of different sub-fractions, the number of modified sites was normalized by the total number of identified peptide spectra matched for albumin (PSM) of the same search run. This allowed for a semi-quantitative comparison based on the degree of modification. As expected, the chromatographic clusters and the pools they represented were not uniformly modified. In healthy controls, each cluster possessed its own characteristic pattern of modification (Supplementary Fig. 2a). Moreover, in all blood samples, the degree of an assortment of modifications correlated well with the NaCl concentration required for AEC elution with respect to the predicted net charge, at least with the major albumin-containing pools that exhibited the highest PSM and sequence coverage. These modifications were carbamoylation (Fig. 5a), deamidation (N, Q: Fig. 5b; R: Fig. 5c), myristoylation (Fig. 5d), and the number of hexoses linked to K (Fig. 5e). Carboxymethylation and carboxyethylation inversely correlated with AEC elution (Fig. 5i). Palmitoylation, palmitoleylation, and methylation show maxima in different sub-fractions (Fig. 5f–h). Moreover, in healthy controls, the intensity of fluorescence related to the advanced glycation end products (AGE) correlated with the ionic strength (Supplementary Fig. 6a) required for elution as well as with carbamoylation and glycation (Supplementary Fig. 6b,c).

Albumin clusters in non-diabetic patients suffering from ESRD had a similar modification pattern (Supplementary Fig. 2b). Of note is the marked elevation of deamidations (Fig. 5b,c), phosphorylation, succinylation (Fig. 5j,k), as were carbamoylation. This was particularly so in sub-fractions originating from the apparently low Mw 1D-fraction (1D 71, Fig. 5a). As expected, AGE-fluorescence intensities were much higher in all sub-fractions from patients than from controls (Supplementary Fig. 6a). In contrast to the situation in healthy people (see above), in patients most of these values do not correlate either with the number of the same modifications per PSM or with carboxymethylation and methylation (Supplementary Fig. 6).

Serum albumin of dog puppies is also heterogeneous in blood plasma. Plasma from puppies had a similar distribution of sub-fractions containing albumin (P49822, Supplementary Fig. 3). The centric Mw was ~6 kDa higher than predicted from the sequence data (Uniprot) as with human albumin. However, because of small volumes, it was not possible to build pools of the residual 2D-fractions. Therefore, we reanalyzed the raw data from single 2D-fractions derived from the centric 1D-fraction 64. These fractions contained several modifications similar to those in human albumin although all to a lower degree: carbamoylation (K) (Fig. 5l), deamidations (N, Q, R) N-glycation (K), methylation (E, D, H), and carboxymethylation (K) and acetylation (T, S, H, Y). With the exception of carbamoylation, these modifications show no clear correlation with AEC-elution. In contrast to the case in samples from human adults, there was no palmitoylation, myristoylation, octanoylation or decanoylation. However, some propionylations on S471 were evident. It should be noted that the degree of carbamoylation of 2 sub-fractions was much higher in puppies with preclinical Alport syndrome (bearing the collagen IV α 5 mutation) than in healthy controls (Fig. 5l).

Albumin in human CSF. In contrast to plasma albumin, the main protein peak in CSF has only one centric Mw of ~78 kDa after 1D-SEC which, as in plasma, was distributed over five 2D-AEC elution steps (Supplementary Fig. 4). After immune quantitation, we were only able to identify a subset of only 4 albumin proteoforms in CSF (Supplementary Fig. 5). These had several modifications, such as carbamoylation (Fig. 5a), glycation (Fig. 5e), and methylation (Fig. 5h), which were correlated with the expected net charge. Nevertheless, these modifications were rarer than in the corresponding albumin forms from plasma. A few deamidations were present but without correlation with 2D-AEC elution (Fig. 5b,c). While one octanoylation (S478) was always present, there was no carboxymethylation and no carboxyethylation, and only very rare palmitoylation and myristoylation.

Discussion

The precision of sample pre-fractionation and proteome coverage of our workflow allows reliable sample comparison for biomarker search. We were therefore able to validate several biomarker candidates by ELISA^{16,17,26,28}. Nevertheless, it was not possible to verify by immune assay some of our other biomarker candidates that appear in one of a multitude of chromatographic clusters^{16,28}. We therefore analyzed the principle and capability of our pre-fractionation in order to determine whether such clusters represent enriched proteoforms varying in, and separated according to, characteristic PTM. To this end we analyzed, as an example, chromatographic clusters of albumin, after 2D-separation. We omitted 3D-separation and the analysis of glycans because albumin is not glycosylated²⁹. Although we still used highly variable protein mixtures for PTM search, albumin represented the main component throughout. Within each search run it was possible to identify not only location but also the

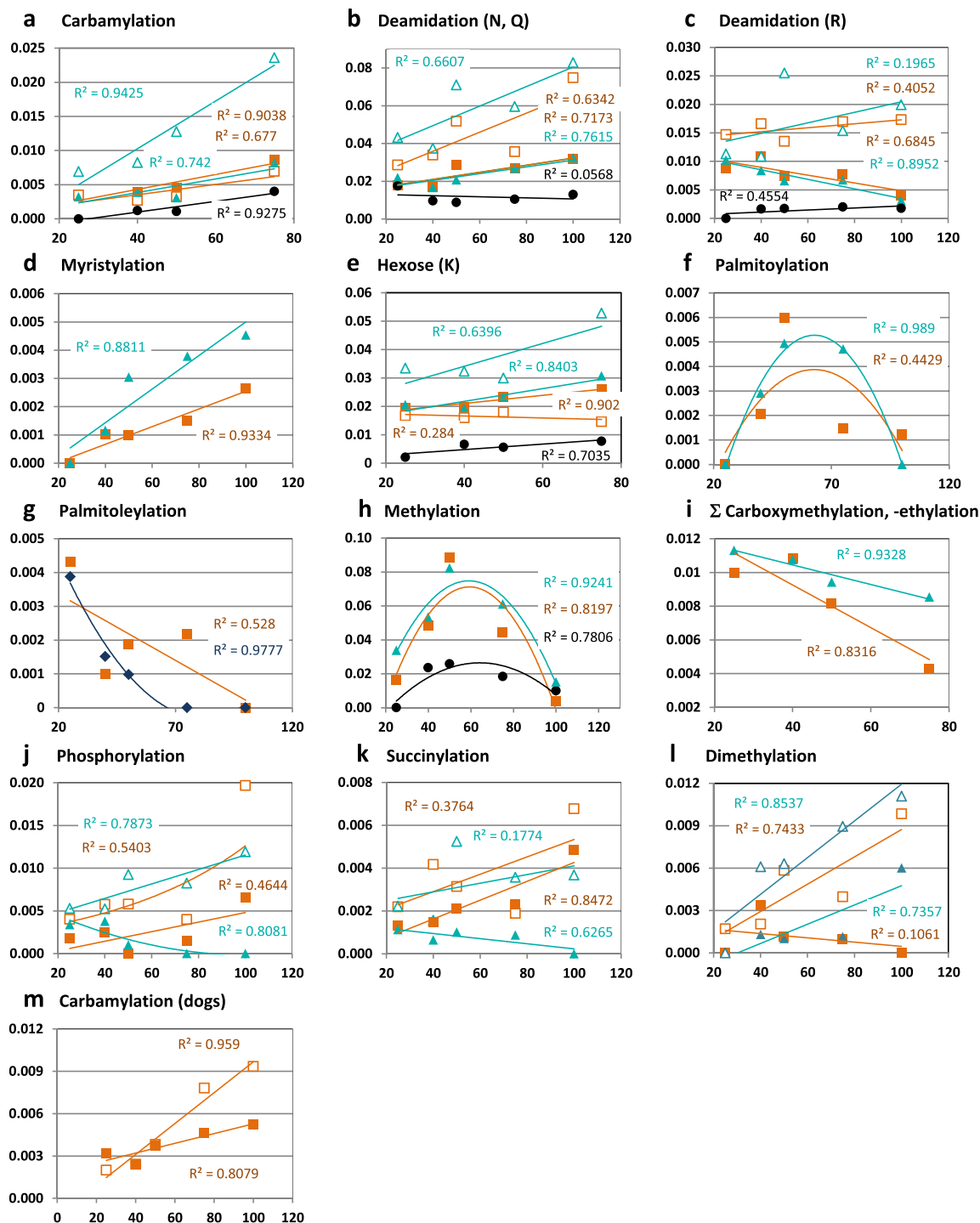


Figure 5. Dependence of the degree of PTM (n PTM/PSM) on the concentration of NaCl required for the elution of albumin from AEC matrix. Filled symbols: healthy plasma volunteers and healthy dogs; open symbols: plasma from patients with ESRD and dogs affected by preclinical Alport syndrome. Sub-fractions from plasma pools: orange squares, sub-fractions derived from albumin centric 1D (human plasma: 1D 67, dog plasma: 1D 23); turquoise triangles, sub-fractions derived from LMW albumin (1D 71); blue diamonds, sub-fractions derived from high Mw albumin (1D 63); black circles, sub-fractions from human CSF albumin, centric 1D 23. Data of human plasma were combined from individually pre-fractionated, prepared and analyzed samples from two healthy male volunteers (multi reports from four runs) and from four patients under hemodialysis (multi reports from eight runs). Due to slightly different pooling of the 2D-fractions, data from healthy male and female volunteers were not combined. Results from healthy female volunteers are similar to those from male volunteers and are shown in Supplementary Fig. 8. Accordingly, data from human CSF represent multi reports of nine runs (three sample pools analyzed in triplicate) and data from dog serum are means of technical duplicates from two sample pools. Ordinates: number of affected sites of the modification per PSM (n PTM/PSM) Abscissas: Concentration of NaCl (mM) required for elution of the sub-fraction from the AEC matrix (cf. Fig. 4c). R^2 is given in the same color as and near to the corresponding data points.

maximum number of occupied or modified sites. However, it was possible to estimate the rate of modification by normalizing these counts with PSM (i.e. the sum of modified and non-modified identified peptides).

The serum albumin of healthy individuals and patients contains several major modifications attributed to micro heterogeneity (oxidation, glycation and S-nitrosylation)^{10,18,30}. Nevertheless, information on the extent and distribution of other modifications is rare. There are, though, two major and seven minor fractions identified and partially characterized by IEX/MS starting from Cohn fraction IV³¹. Our native 2D-fractionation method applied to whole blood plasma shows, however, that the complexity is, in fact, much higher. Serum albumin subdivides into at least 17 different parts all of which are modified in multiple ways. Most of the modifications, with the exception of deamidation, glycation and methylation, affect less than one percent of all the peptides identified (PSM). Nevertheless, their cumulative effect on charge and conformation might produce the characteristic sub-fractions observed. Carbamoylation (K), deamidation (N, Q), and glycation (K) lead to the loss of positive charges³², produce higher negative net charges, and correlate well with the ionic strength necessary for elution from our AEC matrix. In contrast, we found an inverse relationship for carboxymethylation and carboxyethylation (K), although these modifications introduce additional negative charges (Fig. 5i). Carboxylations (K, E, D) surprisingly show no relation to AEC elution. It is possible, therefore, that this is because these modifications either form intramolecular complexes, complexes with other plasma proteins, or complexes with divalent metal ions, thereby altering conformation and the interaction with the AEC matrix. Some known modifications of albumin have a strong influence on the structure and function of albumin^{18,33,34}. All other PTM were present to an even lower degree on various sites and showed no clear relation to AEC-elution. For the first time we identified various acylations of distinct albumin sub-fractions. Although up to 6 fatty acids might bind non-covalently to albumin with high affinity^{29,35}, no covalent lipidation has yet been described in the literature. Nevertheless, N- and O-fatty-acylations occur on intracellular proteins³⁶. Moreover, there is some data on acylated functionally active proteins in blood plasma, such as growth hormone³⁷ and ghrelin³⁸. Acylation can be achieved by both, enzymatic and non-enzymatic^{37,39} and seems to be compatible with water solubility when fatty acids are buried within hydrophobic pockets³⁸, like the non-covalently bound hydrophobic cargo of albumin. It is conceivable that acylation might promote protein-protein interaction. Moreover, we found no S-palmitoylation⁴⁰ (C) probably due to the instability of this bond under DDT reduction before MS³⁷. Albumin acylation still requires verification by other means.

In addition, we re-identified a low degree of carbamoylation in healthy individuals in accordance with a previous study⁴¹ as well as its increase (in a sub-set of our albumin fractions) under renal failure. This modification competes with glycation and is raised under diabetes, chronic kidney diseases, and inflammation^{41,42}. Carbamoylation might occur artificially if urea is present in high concentrations (e.g. for denaturation)⁴³. This is not true for our method and therefore such an artefact is highly improbable.

Deamidation is a common modification of several proteins occurring spontaneously, both *in vivo* and *in vitro*. Non-enzymatic deamidation of Q and N is considered to be both pathological and physiological, increasing protein negative charge, altering conformation, stability, longevity, and function⁴⁴. Although Q is more resistant to deamidation⁴⁴ than N (under physiological conditions its half-life is ten times that of N), we identified Q and N deamidations in similar proportions in our albumin fractions (e.g. mean number/PSM in all pools from healthy males: N, 0.0123; Q, 0.0117). Deamidation (N + Q) shows a strong correlation with AEC elution (Fig. 5b). We cannot exclude, however, that spontaneous N deamidation might be favored to a degree by the conditions of our tryptic digest after protein separation. High pH and temperature, particularly with the use of ammonium bicarbonate, is known to produce this modification⁴⁴. However, because we uniformly applied these conditions to all sub-fractions, the differences identified cannot be explained as artifacts. The degree of R deamidation is higher in ESRD patients than in healthy individuals, but lower than those of Q and N (Fig. 5c). Deamidation converts R into either ornithine or citrulline⁴⁵ thereby altering polarity but not charge. Although this modification can occur spontaneously under alkaline conditions⁴⁵, the sites of deamidation were identical across all analyzed plasma sub-fractions: R264, R343, R542. The degree of oxidation of M correlates well with our AEC elution. Although the oxidation of albumin (C, M) is a common and wide spread reaction⁴⁶ particularly as part of the antioxidant activity of albumin^{47,48} and under oxidative stress in renal diseases⁴⁹, we omitted these data, because we are unable to exclude the possibility of some oxidation during sample preparation. In contrast, glycation is unlikely to result from *ex vivo* reactions⁵⁰, since this non-enzymatic reaction exhibits low binding rate constants and requires high glucose concentration and temperature⁵¹. This reaction is unlikely in our study as all our samples were frozen quickly in liquid nitrogen. Moreover, after 1D-separation (SEC) the proteins were freed from non-bound sugars. Thus the degree of glycation appears to reflect natural modification.

All PTM were primarily identified as mass alteration of peptides by MS. Although distinct mass alterations might be attributed to different PTM, there is currently no alternative to MS for the majority of the PTM we identified. For partial verification we were able to quantify albumin concentration, glycation, and carbamoylation by the ELISA techniques available. The total albumin immune reactivity correlated well with the MS measure “area” for all the albumin peptides identified (Supplementary Fig. 7a) as well as with PSM in the concentration range of the majority of sub-fractions. As expected, PSM values were saturated at high protein concentrations (Supplementary Fig. 7b). However, quite surprisingly, neither the degree of glycation or of carbamoylation by MS was correlated with those determined by ELISA (Supplementary Fig. 7c,d). The percentages of glycation were similar with both methods; carbamoylation was much lower in ELISA than in MS. This illustrates a difficulty; the MS and ELISA results do not refer to exactly the same items. In contrast to ELISA, the MS determination of hexoses included not only glucose but also other sugars of the same Mw without identifying these other sugars. MS quantifies the number of modified residues, ELISA, however, detected the concentration of modified protein molecules. ELISA therefore probably either detected only some of the modifications or identified them independently of the variation in the number of modified sites per protein molecule. Nevertheless, the percentages of the immune reactive glycated albumin protein correlated well with AEC elution (Supplementary Fig. 7e) and

Peak, valley	MW (kDa)	Major components	A ₂₈₀ (mAU)		elution volume (mL)	
			Mean	CV (%)	Mean	CV (%)
I	747.2	lipoproteins	558.8	0.93	49.01	0.00
1			168.0	1.99	54.73	0.12
II	203.2	immunoglobulins	1061.0	1.16	64.41	0.07
2			281.5	2.38	69.63	0.11
III	71.2	transferrin, albumin	1372.1	1.13	76.18	0.08
IV	2.3	intrinsic peptides	28.9	1.03	117.77	0.00
V	1.0	intrinsic peptides	275.92	5.47	127.13	0.06

Table 1. Reproducibility of 1D-SEC. Molecular weights were determined according column calibration¹⁴. For designation of peaks (maxima, I-V) and valleys (minima, 1, 2) see Supplementary Fig. 1. There were three measuring points around each maximum/minimum of each run (15 runs). The means and CV thus covered 45 data points (the same data as in Supplementary Fig. 1).

AGE fluorescence intensities (Supplementary Fig. 7f). The percentages were higher in patients than in controls in accordance with^{52,53}. Moreover, the total amount of albumin determined by ELISA in patients was shifted slightly from little modified to greatly modified entities compared to amounts in healthy people (Supplementary Fig. 5). We were unable to analyze pentosidin formation by our MS equipment, a well-known modification under ESRD⁵⁴. So we tried to quantify this modification by ELISA in order to explain the high AGE fluorescence intensities in samples from patients. However, we were unfortunately unable to do this because our 2D fractions contained protein concentrations at the lowest and most unreliable levels that ELISA is able to detect.

The three apparently different molecular weights of plasma albumin could not be explained by PTM, since MS data does not provide strict stoichiometry. Nevertheless, besides PTM it is also possible that apparently large size proteoforms result from complex formation with members of the “albuminome”⁵⁵. We unfortunately cannot discriminate complex formation from co-elution, since non-covalent, low affinity complexes might be dissolved after 2D-AEC. For example, we were, in fact, able to identify α -1 antitrypsin and vitamin D-binding protein in some sub-fractions co-eluting with albumin (Supplementary Fig. S2a,b) which are well-known to ligate with albumin^{56,57}. In healthy individuals, we can exclude the possibility that huge fragmentation and truncation produced low-molecular weight forms because the sequence coverages of the apparently low and high Mw forms are practically identical. It is probable that different strengths of the interaction with the SEC matrix due to different sets of PTM⁵⁸ might be attributed to different protein conformations producing low apparent Mws. We are not able to exclude nicked but adhering fragments. By such modification no altered Mw might be produced rather than an altered conformation. The allocation of albumin after 2D-AEC unexpectedly does not always follow the estimated net charge (cf. carboxylation and carboxymethylation). Moreover, the distribution into identical sub-fractions from patients and from healthy individuals occurs with different degrees of modification (e.g. deamidation, carbamoylation). Hence, the assignment of proteoforms might depend only in part on net charge but also on different conformations, probably due to a certain modification threshold, pattern or, even, an as yet unrecognized modification.

CSF albumin is heterogeneous and also, to a degree, physicochemically different from that in plasma⁵⁹. Applying our workflow, we were only able to identify only 4 clusters with different degrees of PTM. The degree of carbamoylation (Fig. 5a), glycation (Fig. 5e) and methylation (Fig. 5h) is much lower than in plasma. The degree of acylation is so low that CSF albumin can be considered non-acylated. It is possible to explain these differences between CSF albumin and plasma albumin either by a selective transfer of only a subset of modified proteoforms from plasma into CSF⁶⁰, by the absence of complex formation with the plasma “albuminome” or, probably, by synthesis within the central nervous system.

In contrast to Multiomics by SIMPLEX, the simultaneous profiling of proteins, lipids and other metabolites in initially denatured samples⁶¹, our method provides a native proteoform-resolved measurement addressing PTM and compound adducts. Thus, the separation principle of our workflow, combined with its quality characteristics, reproducibly produces highly distinctive protein fractions. As we demonstrated by example, our workflow is optimally suitable for the detection and analysis of differentially regulated proteoforms. Major proteins, like albumin, can be analyzed directly in sub-fractions from blood plasma as well as from CSF. Some of the albumin PTM we identified coincide with those found elsewhere (see above). Moreover, our precise micro-separation can be used for the native preparation of sufficient amounts of selected minor constituents directly from pre-analyzed sub-fractions. This serves as a prerequisite for their final enrichment and subsequent more reliable characterization by targeted MS or other analytical techniques so as to provide true biomarker candidates and antigens for the development of highly PTM selective immunological assays.

Methods

Plasma samples. We included 4 randomly selected healthy human volunteers (mean age 33.5, SD 5.9 years) and 4 patients (54.5 SD 2.3) with end stage renal failure but without diabetes mellitus. Both groups contained 2 males and 2 females. Nine milliliters of blood were collected by venipuncture into EDTA containers (02.1066.001, Sarstedt Nümbrecht, Germany) and centrifuged at 1500 g * 10 min at room temperature no longer than 30 min after withdrawal¹⁶. Samples from patients were identically obtained immediately before hemodialysis treatment. Dog samples were collected from a colony of dogs with X-linked hereditary nephropathy. These dogs have a naturally occurring, 10 base pair deletion in the gene encoding the α 5 chain of type IV collagen. Samples were

collected from 7-week old unaffected male and female, carrier female, and affected male siblings by jugular venipuncture. Blood was placed into a glass EDTA tube which was immediately placed on ice and centrifuged within 30 minutes of collection at 1500 g * 10 min at 4 °C. After centrifugation, the tubes were placed on ice, and plasma was removed, avoiding the buffy coat interface. The plasma was maintained on ice until frozen at -80 °C within 2 hours of initial blood collection. The samples were stored at -80 °C for two to three weeks before being shipped on dry ice and transferred to long-term liquid nitrogen storage. No freeze-thaw cycle was allowed. Human samples were collected in accordance with ethics agreement 4829-06/2016 (JUH Jena). The informed consent of all participants was obtained. Dog samples were collected in accordance with ethics agreements AUP IACUC 2013-0028 and 2016_0017 (TAMU Texas). The study protocol was reviewed and approved by the Texas A&M University Institutional Animal Care and Use Committee.

CSF samples. We used CSF sample from 26 patients with neurological symptoms. CSF samples were collected in accordance to the ethical agreement 3633-11/2012 (JUH Jena). From all participants 12 mL of CSF were collected in polypropylene tubes (Greiner Bio-One 115261) following standard protocol (of the 12, the first 4 mL were used for laboratory measurements). The samples were kept on ice and immediately centrifuged at the bed side for 10 min. at room temperature (3500 g). Supernatants were aliquoted into cryovials (VWR, 479-1237), shock frozen in liquid nitrogen and stored at -150 °C. The CSF samples were characterized using key laboratory parameters. For MS analysis we used only samples without either blood contamination or blood-brain barrier disturbance. We assessed blood contamination by visual inspection for erythrocyte sediment and barrier disturbance by checking for erythrocytes, total protein, cell count and CSF:serum albumin ratio). To ensure adequate amounts of protein for analysis we created 3 mixtures. Each mixture was made up of equal volumes of CSF samples from 7-10 individuals. These pools were concentrated ~70-95-fold by ultrafiltration (AMICON™ Ultra, MWCO 3 kDa, Merck Millipore), followed by 2D fractionation as described below.

Sample preparation. Pre-fractionation of blood samples was performed according to an existing detailed method for human plasma and serum^{14,16,17}. Briefly, we used a 16/60 Highload Superdex™ 200 column and an Äkta purifier (GE-Healthcare, Munich, Germany) and an automated workstation (laboratory setting, Analytik Jena AG, Fig. 2) for 1D-SEC and 2D-AEC. Initial 1D-SEC fractionation produced 96 1D-fractions of different native molecular weight from about 1 mL plasma. Subsequent 2D-AEC on arrays (Fig. 2d) of self-made microcolumns (Fig. 2h) separated each 1D-fraction into 43 2D-sub-fractions by applying a stepwise elution protocol¹⁴. Human plasma was separated individually. Clusters of albumin containing 2D-fractions of human plasma samples were pooled (Fig. 4c). To obtain sufficient material for the analysis of PTM in puppies we built two sample mixtures (0.75 mL) from unaffected female and affected male dogs. Each mixture contained equal volumes from three individual samples. For the determination of the total number of proteins, four mixtures were built from another set of unaffected male and female, carrier female, and affected male dogs (1.0 mL) from three individual samples each. Pre-fractionation of CSF samples was slightly modified. Briefly, 0.25 mL of mixed and concentrated CSF containing a protein amount of 8 mg (BCA Assay Kit, Pierce, 23227) were 1D-separated on a Superdex 200 GL column (10/300). Thus, 66 fractions of 350 µL each were collected into chilled 96-well deep well plates (flow rate 350 µL/min). Of these, 39 1D-fractions (instead of the 43 for plasma, protein concentration >0.05 mg/mL (A₂₈₀)) were separated by 2D AEC.

Protein recovery from microdialyzers. BSA was quantified by A₂₈₀ and hemoglobin by the cyanhemoglobin reference method.

AGE-fluorescence. Gemini XPS Microplate Reader, Molecular Device (ex 355/em 460 nm, Cutoff 455³⁴) 100 µL sample volume, in microplates (655076, Greiner bio-one).

Mass spectrometry and PTM search. We performed tryptic digest and MS as previously described^{14,16}. Briefly, the separation of tryptic peptides prior to mass spectrometry was performed on a Hypersil Gold UHPLC column (1.9 µm, 50 × 1.0 mm) using an Accela 1250 UHPLC system (both Thermo Fisher Scientific, USA) using binary gradient elution of the mobile phase. This gradient involved 0.1% formic acid in (A) water and in (B) acetonitrile at a flow rate of 150 µL min⁻¹, throughout (0-1 min 5% B, 21 min 30% B, 24 min 40% B, 25 min 90% B, 25.1-26 min 90% B, 26.1-30 min 5% B). Tandem mass spectrometry (MS/MS) measurements were carried out on an LTQ Orbitrap Discovery (Thermo Fisher Scientific, USA) by positive heated electrospray ionization (H-ESI) at a vaporizer temperature of 200 °C. Sheath gas flow (30.0) and auxiliary gas flow (10.0) were used to dry the ionspray. The ionization voltage was set to 4.5 kV and the temperature of the ion transfer tube to 275 °C. The MS/MS system was operated in data-dependent TOP10 mode using 1 microscan. For this purpose, ions were monitored in the LTQ ion trap in full scan centroid mode at m/z 350-1700. The ten most intense ions were run through collision-induced dissociation for further orbitrap high resolution (30,000) analysis (profile data type). Wideband activation was used. The automatic gain control target value for the Orbitrap mass analyzer in full scan mode was 1.0 × 10⁶. The LC-MS/MS was operated via the graphical interface of the Xcalibur software 2.1. Fractions from blood plasma and CSF were run in duplicate and triplicate followed by a blank (water) to avoid carryover. For quality control, a digested transferrin (human (Holo), SERVA Electrophoresis GmbH, 36756, 50 µg mL⁻¹) was analysed four times per microplate.

We considered identical chromatographic 2D-sub-fractions (identical 1D- and 2D-location) to contain identical proteoforms of albumin due to their identical physicochemical properties. Because of this, we were able to combine, when equally pre-fractionated, counts of the PTM of proteins of identical 1D- and 2D-location but from different runs. We built up to 17 pools from 2D-subfractions of each plasma sample containing the major parts of visible albumin clusters. Due to slight differences in pooling of 2D-sub-fractions from healthy individuals, we processed the data sets from the 2 females separately from those of the two males. Although the samples were

processed apart, we combined the data from all 4 patients under hemodialysis (2 females and 2 males) by taking the mean values. These values we then compared with the identically obtained data from the 2 healthy male individuals. CSF and dog plasma albumin were analyzed in MS data of 2D-fractions of known major albumin content without pooling thereby reanalyzing the MS raw data from human CSF and dogs (still unpublished data) from other studies. The search for PTM ran successively using Proteome Discoverer[®] 1.3 (Thermo) with no more than three dynamic modification types per run. We considered only highly confident database matches. The following dynamic modifications of amino acids were analyzed: oxidation (M), palmitoyl (K, S, T), palmitoleyl (S, T), myristoyl (K), octanoyl (S, T), decanoyl (S, T), deamidation (N, Q, R), carboxy (D, E, K, W), carboxymethyl (K, W), carboxyethyl (K), carbamoyl (K, M, R), hexose (K, N, R, T, W, Y), acetyl (H, K, S, T, Y), ethyl (E, K), dimethyl (K, N, R), propionyl (K, S), methyl (D, E, H, I, K, L, N), phosphoryl (S, T, Y), and succinyl (K). Multi reports of the related replicates were utilized.

ELISA. Albumin was measured using a slight modification of an existing method²⁶. Briefly, 25 μ L of the samples and the standards were incubated for 90 min. at room temperature in the wells of 384-well microplates (781094, Greiner bio-one) pre-coated with anti-human albumin (1.0 μ g/mL (rabbit, DAKO) overnight at 4 °C). After washing (seven times, 100 μ L) the wells were incubated with 25 μ L goat anti-human albumin-HRP conjugate (1:20.000, A80-2299, Bethyl Lab.) for 2 h. After washing, 25 μ L of substrate were added (TMB X-tra, Biotrend: #4800 H) and the reaction was stopped by 25 μ L 0.5 M H₂SO₄ after ~20 min and visual inspection. Due to the limited sample volumes and protein concentrations, it was only possible to analyze the 8 most highly concentrated 2D-pools (67.1 to 67.4, 71.1 to 71.4) by PTM-selective ELISA according to the instruction of the suppliers. We tested all selected 2D-pools in duplicate with deviations of no more than 10%. Carbamoylation: Human Carbamylated Albumin ELISA (XPEH0930) supplied by XpressBio; 1 to 5 and 1 to 10 diluted 2D-pools. Pentosidine: Human Pentosidine ELISA-Kit (CSB-E09415h) from Cusabio[®] applying 1 to 5 diluted 2D-pools. Glycation: Glycated human albumin competitive ELISA-Kit (CSB-E09599h) from Cusabio[®]; slightly modified: we pre-mixed 2D-pools (diluted 1 to 3) and conjugate solutions before spotting to the wells.

References

1. Drabovich, A. P., Martinez-Morillo, E. & Diamandis, E. P. Toward an integrated pipeline for protein biomarker development. *Biochim Biophys Acta* **1854**, 677–686 (2015).
2. Khalilpour, A., Kilib, T., Khalilpour, S., Alvarez, M. M. & Yazdi, I. K. Proteomic-based biomarker discovery for development of next generation diagnostics. *Appl Microbiol Biotechnol* **101**, 475–491 (2017).
3. Matthews, H., Hanison, J. & Nirmalan, N. “Omics”-Informed Drug and Biomarker Discovery: Opportunities, Challenges and Future Perspectives. *Proteomes* **4** (2016).
4. Krüger, T., Lehmann, T. & Rhode, H. Effect of quality characteristics of single sample preparation steps in the precision and coverage of proteomic studies—a review. *Anal Chim Acta* **776**, 1–10 (2013).
5. Ioannidis, J. P. A. & Bossuyt, P. M. M. Waste, Leaks, and Failures in the Biomarker Pipeline. *Clin Chem* **63**, 963–972 (2017).
6. Büchler, R., Wendler, S., Muckova, P., Grosskreutz, J. & Rhode, H. The intricacy of biomarker complexity—the identification of a genuine proteomic biomarker is more complicated than believed. *Proteomics Clin Appl* **10**, 1073–1076 (2016).
7. Schrödl, W. *et al.* Acute phase proteins as promising biomarkers: Perspectives and limitations for human and veterinary medicine. *Proteomics Clin Appl* **10**, 1077–1092 (2016).
8. Smith, L. M. & Kelleher, N. L., Consortium for Top Down, P. Proteoform: a single term describing protein complexity. *Nat Methods* **10**, 186–187 (2013).
9. Agrawal, S. & Smoyer, W. E. Role of albumin and its modifications in glomerular injury. *Pflugers Arch* **469**, 975–982 (2017).
10. Magzal, F. *et al.* *In-vivo* oxidized albumin- a pro-inflammatory agent in hypoalbuminemia. *PLoS One* **12**, e0177799 (2017).
11. Aebersold, R. *et al.* How many human proteoforms are there? *Nat Chem Biol* **14**, 206–214 (2018).
12. Cerny, M., Skalak, J., Cerna, H. & Brzobohaty, B. Advances in purification and separation of posttranslationally modified proteins. *J Proteomics* **92**, 2–27 (2013).
13. Naryzhny, S. Inventory of proteoforms as a current challenge of proteomics: Some technical aspects. *J Proteomics* **191**, 22–28 (2019).
14. Wendler, S. *et al.* In *Automations Systems of the 21st Century*. (ed. D. Arent, Freebush, M.) 1–50, open access. (nova publishers, New York; 2013).
15. Horn, A. *et al.* Multidimensional proteomics of human serum using parallel chromatography of native constituents and microplate technology. *Proteomics* **6**, 559–570 (2006).
16. Reindl, J. *et al.* Proteomic biomarkers for psoriasis and psoriasis arthritis. *J Proteomics* **140**, 55–61 (2016).
17. Muckova, P. *et al.* Preclinical Alterations in the Serum of COL(IV)A3(–)/(–) Mice as Early Biomarkers of Alport Syndrome. *J Proteome Res* **14**, 5202–5214 (2015).
18. Maciazek-Jurczyk, M., Szkudlarek, A., Chudzik, M., Pozycka, J. & Sulkowska, A. Alteration of human serum albumin binding properties induced by modifications: A review. *Spectrochim Acta A Mol Biomol Spectrosc* **188**, 675–683 (2018).
19. Büschel, M., Sammler, G., Tautkus, B., Wendler, S. & Rhode, H. Micro sample container and method for pouring in liquid samples into a micro sample container. Patent application. EP16171567.7. (ed. U.H. Jena) (Germany; 2016).
20. Maischak, H., Tautkus, B., Kreuzsch, S. & Rhode, H. Proteomic sample preparation by microdialysis: easy, speedy, and nonselective. *Anal Biochem* **424**, 184–186 (2012).
21. Rhode, H. *et al.* Device for receiving, treating, and storing of small volume samples. Patent application. DE102007011866. (ed. U.H. Jena) (Germany; 2008).
22. Kreuzsch, S. *et al.* Searching biomarker candidates in serum using multidimensional native chromatography. I. Enhanced separation method. *J Chromatogr B Analyt Technol Biomed Life Sci* **875**, 567–572 (2008).
23. Xue, L. *et al.* Mixed-mode ion exchange-based integrated proteomics technology for fast and deep plasma proteome profiling. *J Chromatogr A* **1564**, 76–84 (2018).
24. Gegotek, A., Domingues, P., Wronski, A., Wojcik, P. & Skrzydlewska, E. Proteomic plasma profile of psoriatic patients. *J Pharm Biomed Anal* **155**, 185–193 (2018).
25. Opsahl, J. A. *et al.* Label-free analysis of human cerebrospinal fluid addressing various normalization strategies and revealing protein groups affected by multiple sclerosis. *Proteomics* **16**, 1154–1165 (2016).
26. Baum, A. *et al.* Searching biomarker candidates in serum using multidimensional native chromatography. II Method evaluation with Alport syndrome and severe inflammation. *J Chromatogr B Analyt Technol Biomed Life Sci* **876**, 31–40 (2008).
27. Hallbauer, J., Kreuzsch, S., Klemm, A., Wolf, G. & Rhode, H. Long-term serum proteomes are quite similar under high- and low-flux hemodialysis treatment. *Proteomics Clin Appl* **4**, 953–961 (2010).
28. Pohl, M. *et al.* Diagnosis of Alport syndrome—search for proteomic biomarkers in body fluids. *Pediatr Nephrol* **28**, 2117–2123 (2013).

29. Fasano, M. *et al.* The extraordinary ligand binding properties of human serum albumin. *IUBMB Life* **57**, 787–796 (2005).
30. Watanabe, H., Imafuku, T., Otagiri, M. & Maruyama, T. Clinical Implications Associated With the Posttranslational Modification-Induced Functional Impairment of Albumin in Oxidative Stress-Related Diseases. *J Pharm Sci* **106**, 2195–2203 (2017).
31. Leblanc, Y., Bihoreau, N. & Chevreux, G. Characterization of Human Serum Albumin isoforms by ion exchange chromatography coupled on-line to native mass spectrometry. *J Chromatogr B Analyt Technol Biomed Life Sci* **1095**, 87–93 (2018).
32. Kalim, S., Karumanchi, S. A., Thadhani, R. I. & Berg, A. H. Protein carbamylation in kidney disease: pathogenesis and clinical implications. *Am J Kidney Dis* **64**, 793–803 (2014).
33. Lee, P. & Wu, X. Review: modifications of human serum albumin and their binding effect. *Curr Pharm Des* **21**, 1862–1865 (2015).
34. Raghav, A., Ahmad, J., Alam, K. & Khan, A. U. New insights into non-enzymatic glycation of human serum albumin biopolymer: A study to unveil its impaired structure and function. *Int J Biol Macromol* **101**, 84–99 (2017).
35. Oran, I. & Oran, B. Ischemia-Modified Albumin as a Marker of Acute Coronary Syndrome: The Case for Revising the Concept of “N-Terminal Modification” to “Fatty Acid Occupation” of Albumin. *Dis Markers* **2017**(), 5692583 (2017).
36. Chen, B., Sun, Y., Niu, J., Jarugumilli, G. K. & Wu, X. Protein Lipidation in Cell Signaling and Diseases: Function, Regulation, and Therapeutic Opportunities. *Cell Chem Biol* **25**, 817–831 (2018).
37. Hentschel, A., Zahedi, R. P. & Ahrends, R. Protein lipid modifications—More than just a greasy ballast. *Proteomics* **16**, 759–782 (2016).
38. Resh, M. D. Fatty acylation of proteins: The long and the short of it. *Prog Lipid Res* **63**, 120–131 (2016).
39. Harmel, R. & Fiedler, D. Features and regulation of non-enzymatic post-translational modifications. *Nat Chem Biol* **14**, 244–252 (2018).
40. Peng, T., Thinon, E. & Hang, H. C. Proteomic analysis of fatty-acylated proteins. *Curr Opin Chem Biol* **30**, 77–86 (2016).
41. Nicolas, C. *et al.* Carbamylation is a competitor of glycation for protein modification *in vivo*. *Diabetes Metab* **44**, 160–167 (2018).
42. Delanghe, S. *et al.* Quantification of carbamylated albumin in serum based on capillary electrophoresis. *Electrophoresis* **38**, 2135–2140 (2017).
43. Kollipara, L. & Zahedi, R. P. Protein carbamylation: *in vivo* modification or *in vitro* artefact? *Proteomics* **13**, 941–944 (2013).
44. Hao, P., Adav, S. S., Gallart-Palau, X. & Sze, S. K. Recent advances in mass spectrometric analysis of protein deamidation. *Mass Spectrom Rev* **36**, 677–692 (2017).
45. Reubsaet, J. L. *et al.* Analytical techniques used to study the degradation of proteins and peptides: physical instability. *J Pharm Biomed Anal* **17**, 979–984 (1998).
46. Davies, M. J. Protein oxidation and peroxidation. *Biochem J* **473**, 805–825 (2016).
47. Drazic, A. & Winter, J. The physiological role of reversible methionine oxidation. *Biochim Biophys Acta* **1844**, 1367–1382 (2014).
48. Rosenfeld, M. A., Vasilyeva, A. D., Yurina, L. V. & Bychkova, A. V. Oxidation of proteins: is it a programmed process? *Free Radic Res* **52**, 14–38 (2018).
49. Suzuki, S. *et al.* Methionine sulfoxides in serum proteins as potential clinical biomarkers of oxidative stress. *Sci Rep* **6**, 38299 (2016).
50. Jeffs, J. W., Ferdosi, S., Yassine, H. N. & Borges, C. R. *Ex vivo* instability of glycated albumin: A role for autoxidative glycation. *Arch Biochem Biophys* **629**, 36–42 (2017).
51. Anguizola, J. *et al.* Review: Glycation of human serum albumin. *Clin Chim Acta* **425**, 64–76 (2013).
52. Akalin, N., Koroglu, M., Harmankaya, O., Akay, H. & Kumbasar, B. Comparison of insulin resistance in the various stages of chronic kidney disease and inflammation. *Ren Fail* **37**, 237–240 (2015).
53. Guthoff, M. *et al.* Impact of end-stage renal disease on glucose metabolism—a matched cohort analysis. *Nephrol Dial Transplant* **32**, 670–676 (2017).
54. Miyata, T., van Ypersele de Strihou, C., Kurokawa, K. & Baynes, J. W. Alterations in nonenzymatic biochemistry in uremia: origin and significance of “carbonyl stress” in long-term uremic complications. *Kidney Int* **55**, 389–399 (1999).
55. Liu, Z. *et al.* Proteomic and network analysis of human serum albuminome by integrated use of quick crosslinking and two-step precipitation. *Sci Rep* **7**, 9856 (2017).
56. Scumaci, D. *et al.* Assessment of an ad hoc procedure for isolation and characterization of human albuminome. *Anal Biochem* **418**, 161–163 (2011).
57. Gundry, R. L., Fu, Q., Jelinek, C. A., Van Eyk, J. E. & Cotter, R. J. Investigation of an albumin-enriched fraction of human serum and its albuminome. *Proteomics Clin Appl* **1**, 73–88 (2007).
58. Wagner, M. C. *et al.* Mechanism of increased clearance of glycated albumin by proximal tubule cells. *Am J Physiol Renal Physiol* **310**, F1089–F1102 (2016).
59. Bruschi, M., Santucci, L., Candiano, G. & Ghiggeri, G. M. Albumin heterogeneity in low-abundance fluids. *The case of urine and cerebro-spinal fluid*. *Biochim Biophys Acta* **1830**, 5503–5508 (2013).
60. Liddelow, S. A. *et al.* Cellular specificity of the blood-CSF barrier for albumin transfer across the choroid plexus epithelium. *PLoS One* **9**, e106592 (2014).
61. Coman, C. *et al.* Simultaneous Metabolite, Protein, Lipid Extraction (SIMPLEX): A Combinatorial Multimolecular Omics Approach for Systems Biology. *Mol Cell Proteomics* **15**, 1453–1466 (2016).

Acknowledgements

Financial support: Thuringia Ministry for Education, Science and Culture and the EFRE-fund (SW, PM, RB, HR: 2010 FE 9001, 2013 FE 9075, PR: 2013 FE 9077); Federal Ministry for Education and Research (PM: 01GM1304), Federal Ministry for Economic Affairs and Energy and the Central Innovation Program SME (RB, HR, KF 2937601FR1), and Prof. B. Qualmann (MS maintenance). Dr. A. J. Davis of English Experience Language Services, Goettingen, edited versions of the manuscript during its preparation.

Author Contributions

H.R. conceived the experimental design, most of the design of the tools developed, performed the MS analysis of the sub-fractions containing albumin, searched databases for PTM, and drafted the manuscript and figures. P.M. collected, prepared and carried out MS analysis of CSF. B.T. and S.W. performed several experimental steps of pre-fractionation and MS. M.V. contributed the pre-fractionation and tryptic digest of hundreds of sub-fractions and photographed the tools. R.B. contributed the development and comprehensive characterization of microdialyzers and initiated PTM analysis. T.M. contributed technical and robotic solutions. J.G. provided CSF samples and edited the manuscript. A.K. provided plasma samples from patients suffering from ESRD and corrected the manuscript. M.N. provided plasma samples from dogs and edited the manuscript.

Additional Information

Supplementary information accompanies this paper at <https://doi.org/10.1038/s41598-019-48278-y>.

Competing Interests: The authors declare no competing interests.

Publisher's note: Springer Nature remains neutral with regard to jurisdictional claims in published maps and institutional affiliations.



Open Access This article is licensed under a Creative Commons Attribution 4.0 International License, which permits use, sharing, adaptation, distribution and reproduction in any medium or format, as long as you give appropriate credit to the original author(s) and the source, provide a link to the Creative Commons license, and indicate if changes were made. The images or other third party material in this article are included in the article's Creative Commons license, unless indicated otherwise in a credit line to the material. If material is not included in the article's Creative Commons license and your intended use is not permitted by statutory regulation or exceeds the permitted use, you will need to obtain permission directly from the copyright holder. To view a copy of this license, visit <http://creativecommons.org/licenses/by/4.0/>.

© The Author(s) 2019